Gaussian Beam Decomposition of High Frequency Wave Fields

Nicolay M. Tanushev*, Björn Engquist, Richard Tsai

Department of Mathematics
The University of Texas at Austin
Austin, TX 78712

April 22, 2009

Abstract

In this paper, we present a method of decomposing a highly oscillatory wave field into a superposition of Gaussian beams. The goal is to extract the necessary parameters for a Gaussian beam superposition from this wave field, so that further evolution of the high frequency waves can be computed by the method of Gaussian beams. The methodology is described for $\mathbb{R}^d$ with numerical examples for $d = 2$. In the first example, a field generated by an interface reflection of Gaussian beams is deco. The beam parameters are reconstructed to a very high accuracy. The data in the second example is not a superposition of a finite number of Gaussian beams. The wave field to be approximated is generated by a finite difference method for a geometry with two slits. The accuracy in the decomposition increases monotonically with the number of beams.

1 Introduction

We consider the wave equation for $x \in \mathbb{R}^d$,

$$\begin{aligned} \Box u \equiv \partial_{tt} u - c(x) \triangle u &= 0 , & t > 0 \\ u &= f(x) , & t = 0 \\ \partial_t u &= g(x) , & t = 0 . \end{aligned} \tag{1}$$

This equation is well posed in the energy norm,

$$||u||_E = \left(\int_{\mathbb{R}^d} \left[\frac{1}{c(x)} |u_t|^2 + |\nabla u|^2 \right] dx \right)^{1/2} ,$$

where ∇ is the gradient with respect to the spacial variables.

High frequency solutions to this equation are necessary in many scientific applications. While the equation has no scale, "high frequency" in this case means that there is a scale separation between the wave length and the domain of interest and that the sound speed $c(x)$ does not greatly vary on the scale of the oscillations. In such situations, direct discretization methods are notoriously computationally costly. To circumvent this, one often relies on asymptotically valid approximations such as geometric optics [7], geometrical theory of diffraction [11], and Gaussian beams [2, 8, 9, 10, 16].

To set notation and remind the reader of the high frequency methods that this paper is focused on, we briefly review geometric optics and Gaussian beams. For a more detailed description of Gaussian beams with the similar notation, we refer the reader to [14, 15]. In the high frequency limit with k the large high frequency parameter, one can look for special solutions of the wave equation that take the geometric optics form,

$$u(x,t) \sim a(x,t) e^{ik\phi(x,t)} . \tag{2}$$

* *Email:* nicktan@math.utexas.edu

Then, solving the wave equation is reduced to determining the amplitude function $a(x,t)$ and the phase function $\phi(x,t)$. Upon substituting this ansatz (2) into the wave equation and collecting like powers of k, one obtains eikonal equation for the phase and the transport equation for the amplitude,

$$\begin{aligned} |\phi_t|^2 - c(x)|\nabla\phi|^2 &= 0 \\ 2\phi_t a_t - 2c(x)\nabla\phi\cdot\nabla a &= -a\Box\phi \ . \end{aligned}$$

In the method of geometric optics, these equations are solved by PDE techniques or by ODE ray tracing [7] for a real value phase and amplitude. Alternatively, in the Gaussian beams method, one relaxes the conditions on ϕ and a to allow them to take on complex values and one expresses them as Taylor polynomials about a characteristic ray, $(\mathcal{X}(s),\mathcal{T}(s))$, that originates at some point $(y,0)$ with ray parameter s:

$$\begin{aligned} \phi(x,t;y,s) &= \Phi(s) + \Phi_t(s)(t-\mathcal{T}) + \nabla\Phi(s)\cdot(x-\mathcal{X}) \\ &\quad + \frac{1}{2}[(x,t)-(\mathcal{X},\mathcal{T})]\cdot Hess[\Phi](s)[(\mathcal{X},\mathcal{T})-(x,t)] \qquad (3) \\ a(x,t;y,s) &= A(s) \ . \qquad (4) \end{aligned}$$

Here, $Hess[\Phi]$ is Hessian matrix of Φ (which includes the second order x and t derivatives) and the above coefficients are defined through the ray tracing system of ODEs (using the shorthand notation $\tau = \Phi_t$, $\xi = \nabla\Phi$, $M = Hess[\Phi]$ and $\dot{} = \frac{d}{ds}$) :

$$\begin{aligned} \dot{\mathcal{T}} &= 2\tau \\ \dot{\mathcal{X}} &= -2c(x)\xi \\ \dot{\tau} &= 0 \\ \dot{\xi} &= |\xi|^2\nabla c \\ \dot{\Phi} &= 0 \\ \dot{M} &= -MDM - MB - B^tM - C \\ \dot{A} &= -A\Box\Phi \end{aligned}$$

The matrices B, C, and D are $(d+1)\times(d+1)$ dimensional and defined as derivatives of $p(x,t,\xi,\tau) = |\tau|^2 - c(x)|\xi|^2$:

$$(B)_{kl} = \frac{\partial^2 p}{\partial\zeta_k\partial z_l} \qquad (C)_{kl} = \frac{\partial^2 p}{\partial z_k\partial z_l} \qquad (D)_{kl} = \frac{\partial^2 p}{\partial\zeta_k\partial\zeta_l} \ ,$$

with $z=(x,t)$ and $\zeta=(\xi,\tau)$. Thus defined, ϕ and a do not satisfy the eikonal and transport equation exactly, except on the ray; nonetheless, u given by equation (2) will be an asymptotic solution of the wave equation (see [14, 15]).

To obtain a Gaussian beam solution, one has to determine the Taylor coefficients and the initial beam center y. Note that due to the relations between these coefficients that the eikonal equation (and its derivatives) provide, one only needs to determine the derivatives that involve x to determine all of the coefficients (up to the sign of ϕ_t). Also, although in the expression for ϕ and a both s and t appear as separate parameters, they are related through the condition $\mathcal{T}(s) = t$. What makes this type of construction give a valid asymptotic solution to the wave equation is that the x derivative block of the imaginary part of the Hessian matrix is a positive definite matrix. One can show that if this condition holds at $t=0$, it will hold for all t, see [14]. This gives the name of the method, as at any given t the magnitude of the solution has a Gaussian shape.

Whether one uses geometric optics or Gaussian beams, an important fact to recognize is that the initial data for the wave equation, f and g in equation (1), have to fit with the special form of the solution. For geometric optics we need the initial data to top order in k to be of the form, $f(x) = a(x)\exp(ik\phi(x))$, with real valued phase ϕ, while for Gaussian beams, we need it to be $f(x) = a(x;y)\exp(ik\phi(x;y))$, where a and ϕ given by Taylor expansions about y. To see the required form for g, one recognizes that a and ϕ are functions of t as well and differentiates.

Finally, one can exploit the linear nature of the wave equation by finding the solution for N different initial data. Adding these together gives a solution to the wave equation with initial data given by the sum of their individual initial data. For the case of Gaussian beams, this means that the solution we can obtain has initial data of the form,

$$\sum_{n=1}^{N} a_n(x;y_n)e^{ik\phi_n(x;y_n)} \ .$$

In many applications, the available data is not typically in form required to for geometric optics or Gaussian beams. Thus we need to re-represent it in the appropriate from. A common method is to represent the field using the Fourier transform, so that it is in the form of an amplitude function times an exponential involving a phase [9, 16]. This approach has some drawbacks as the number of distinct phases can be quite large, since this representation relies on strong cancellations to represent the field. One then has to propagate the field for every distinct phase, thus leading to a computationally complex method. For geometrical optics, the authors of [1] give a method for decomposing a time harmonic wave field at a particular point into several plane waves, which eliminates some of these difficulties. The method in [1] is related to our approach as the authors also use the Fourier transform and look for maximums of a function to find the oscillation directions. They also assume no knowledge of the number of distinct phases. However, our objectives differ, as we are aiming to have a representation of the entire field, not just at a single point. Also, our basic building blocks (ie the Gaussian beams) have more parameters that define them. For further references see [1].

For Gaussian beams, some work has also been done in this direction [12, 17]. In [17], the author considers the related problem of representing boundary data for the wave equation as a superposition of beam-like packets. The main tool is to take an integral superposition of beam-like packets and then find under what assumptions the integral superposition agrees with the given boundary data. In turn, these assumptions are used to determine the beam parameters. This results in a collection of beams that propagate in all directions from every point. The method that we propose is formulated for decomposing initial data, and the number propagation directions is governed by the complexity of the wave field and determined automatically by the algorithm. Similarly, in [12], the author considers a Gaussian beam decomposition of an initial time harmonic field, however, the field is assumed to be separated into an amplitude and a phase.

In this paper, we propose a method for approximating the initial data (f, g) for the wave equation by a superposition of Gaussian beams. Our task is to find the number of beams N and their parameters, so that with

$$w(x,t) \quad = \quad \sum_{n=1}^{N} a_n(x,t;y_n) e^{ik\phi_n(x,t;y_n)} \ ,$$

the energy norm,

$$\left(\int_{\mathbb{R}^d} \left[\frac{1}{c(x)} |g - w_t|_{t=0}|^2 + |\nabla (f - w|_{t=0})|^2 \right] dx \right)^{1/2} \ ,$$

is small. We work in this norm, since the wave equation is well posed in it. We use the "energy" function,

$$F[u](x,t) \quad = \quad \frac{1}{c(x)} |u_t|^2 + |\nabla u|^2 \ , \tag{5}$$

and define the related inner product,

$$< u, v >_E \quad = \quad \int_{\mathbb{R}^d} \left[\frac{1}{c(x)} u_t \bar{v}_t + \nabla u \cdot \nabla \bar{v} \right] dx \ .$$

The motivation behind this paper is the practical application of Gaussian beam techniques, for example, in exploration seismology, [9, 8]. There are two important cases for which the methods of this paper apply. One case is the initialization of Gaussian beams – given a wave field, its decomposition into Gaussian beams for computation of the wave field migration imaging process. The other case, arises in simulations when the Gaussian beam approximation is not adequate in a small region of the computational domain due to, for example, sharp local variations in the sound speed. The methods we derive can be used for coupling Gaussian beams to a local approximation of finite difference or finite element type. These applications to exploration seismology will be presented in a forthcoming paper, [5].

2 Method

The method that we propose is iterative and the procedure can be summarized as follows. By performing calculations on the wave field, we find an initial guess for the parameters that define a Gaussian beam. We then optimize these beam parameters locally with constraints to minimize the difference between the Gaussian beam and the wave field in the energy norm. After subtracting the Gaussian beam from the wave field, we repeat the procedure with this new field with reduced energy. The details of these steps are outlined below.

1. With $n = 1$, let (u^n, u_t^n) be the initial field at a fixed t.
2. Estimate Gaussian beam parameters
   - Estimate Gaussian beam center
     - Compute $E^n(x) = |u_t^n|^2 + |\nabla u^n|^2$
     - Let $y_n = \arg\max\{E^n(x)\}$.
   - Estimate propagation direction
     - Let $G(x) = \exp(-k|x - y_n|^2/2)$
     - Let $\nabla\phi_n = \arg\max\{|\mathcal{F}[u(x)G(x)]| + |\mathcal{F}[u_t(x)G(x)/k]|\}$, where $\mathcal{F}$ is the Fourier transform.
   - Set all other Gaussian beam parameters – $D^2\phi_n$ is the Hessian matrix of second x-derivatives of ϕ_n
     - Let $\mathrm{Re}\left\{D^2\phi_n\right\} = 0$
     - Let $\mathrm{Im}\left\{D^2\phi_n\right\} = I$, where I is the identity matrix.
3. Minimize the difference between the Gaussian beam and u^n in the energy norm using y_n, $\nabla\phi_n$, and $D^2\phi_n$ as the initial Gaussian beam parameters.
   - Let $B^n(x,t)$, be the Gaussian beam defined these parameters with amplitude 1 (see formula (3)).
   - Let $a_n = \frac{<u^n, B^n>_E}{||B^n||_E^2}$
   - Let $(\tilde{y}_n, \nabla\tilde{\phi}_n, D^2\tilde{\phi}_n, \tilde{a}_n) = \arg\min\{||u - \tilde{a}^n\tilde{B}^n||_E^2\}$. Take these are the parameters that define the n-th Gaussian beam.
4. Subtract the Gaussian beam field: $u^{n+1} = u^n - \tilde{a}_n\tilde{B}^n$ and $u_t^{n+1} = u_t^n - \tilde{a}_n\tilde{B}_t^n$.
5. Repeat steps starting with step 2, until $||u^{n+1}||_E$ is small

We provide discussion and justification for these steps. Looking at the energy function (5) for a single Gaussian beam, we see that it is a Gaussian distribution with variance $1/k$ and so, the effective range for a Gaussian beam is on the order of $1/\sqrt{k}$ near its center y. Thus, if we want to represent the wave energy at a particular point, we need a Gaussian beam be centered in a small neighborhood of it. Once we have localized near this point, only the local oscillation are relevant, thus we take the Fourier transform of the field with a Gaussian weight and look for a maximum. This Fourier transform can be taken only locally, thus it can be done efficiently. The estimated values for the Hessian come from the fact that we need the imaginary part to be positive definite and that the coefficients are not allowed to be very big, as otherwise the premise of separation of different scales that is necessary for the asymptotic expansion would be violated. Once we have determined the parameters that define the phase function, we can define $B(x,t) = \exp(ik\phi(x,t;y))$ and think of it as a basis function. The appropriate coefficient for representing a field, u, with this function alone is

$$a = \frac{< u, B >_E}{||B||_E^2} \ . \tag{6}$$

This procedure for defining a works because the ODE that defines the evolution of a is homogeneous and, hence, changing the Gaussian beam amplitude can be accomplished simply by multiplication.

One point that should be addressed is that the function $F[u](x)$ can be small in at a point where it would be advantageous to have a Gaussian beam center. Consider, as an example, the case of two beams with the same center y, $\nabla\phi$ which are perpendicular, and amplitudes with opposite signs. At y, the two beams interfere destructively, making the energy function small. For this reason, we need to use the argument maximum of the energy only as an estimate of the Gaussian beam center. In this example, the two Gaussian beams will interfere constructively close to y leading to a good initial estimate for the Gaussian beam centers.

To determine the final Gaussian beam parameters, we minimize the energy norm difference between the Gaussian beam and the wave field. This is a constrained minimization in high dimensional space – there are 11 parameters in 2D and 19 parameters in 3D. The constraints are that the imaginary part of $D^2\phi$ has to be positive definite and that ϕ_t can be determined up to a sign by $|\nabla\phi|$. We note that to maintain the validity of the asymptotic expansion, the coefficients must not be too large. There are several ways to carry out this constrained minimization numerically, including the Nelder-Mead method [13], which was used in the examples below.

To improve the results one can also re-optimize the beams that have been previously extracted by the algorithm with the addition of every new beam, by inserting one or both of the following steps before the "repeat" step in the above algorithm.

(a) If desired, readjust the previous beams with the addition of new beams

- For the j-th beam, let $w = u^{n+1} + \tilde{a}_j \tilde{B}^j$ and repeat step 3 with $u^n = w$, $n = j$, and $(\tilde{y}_j, \nabla\tilde{\phi}_j, D^2\tilde{\phi}_j)$ as the initial Gaussian beam parameters.
- Let $u^{n+1} = w - \tilde{a}_j \tilde{B}^j$

(b) If desired, readjust all beam amplitudes together

- Let D be the matrix of inner products $D_{jl} =< \tilde{B}^l, \tilde{B}^j >_E$, and $b_j =< u^1, \tilde{B}^j >_E$
- Solve $D\tilde{a} = b$ and let $u^{n+1} = u^1 - \sum_{j=1}^n \tilde{a}_j \tilde{B}^j$

For Gaussian beams that represent general wave fields, the optimal results follow if the Gaussian beam parameters for all beams are adjusted at the same time to minimize the energy difference. An optimization involving all beam parameters is computationally prohibitive and the method steps (a) and (b) above can be seen as a practical approximation to full optimization. One can think of step (a) as an alternating minimization step over beams that overlap. Note that this step is not necessary for beams that are well separated. In the same sense, step (b) can be thought of as an adjustment step that minimizes the energy using all of the amplitudes at the same time. It is also the coefficient calculation in writing the wave field in the basis defined by the Gaussian beams in the energy innerproduct.

Another necessary improvement of the basic algorithm is to introduce constraints in the optimization to maintain the positive definiteness of $D^2\phi$ and to ensure that the Gaussian beam coefficients are not too large. For practical purposes, one can require that the coefficients be smaller then $\sqrt{k}$ in magnitude.

2.1 Algorithm Analysis

It is not obvious that the proposed minimization will lead to a global minimum. Thus, to examine this minimization in greater detail, we consider the case when the initial wave field is given by a single Gaussian beam in 1D for the constant coefficient wave equation. The analytic Gaussian beam solution is easily determined in this case as

$$a_0 e^{ik\left[\xi_0(x-x_0\pm t)+\beta(x-x_0\pm t)^2/2\right]} .$$

We study the case of offsetting two beams and examining the difference in the wave fields. The second column of graphs in Figure 1 show the energy landscape in which we are minimizing as y varies (all other parameters are held constant at the exact values of the initial wave field Gaussian beam). First, the Gaussian beam coefficient a is held constant and second, it is defined by equation (6). As the graph shows, in the first case there are several local minima, while in the second case there is only the global minimum. One can think of a as aligning the oscillations of the two beams, as the first column of graphs in Figure 1 shows. This shows why using equation (6) to define a is absolutely necessary. Note that with this choice of a, the energy of the initial wave field minus the wave field of the Gaussian beam will never be greater than the energy of the initial wave field. Thus, the energy difference between the wave field and the Gaussian beam, ie the quantity that we are minimizing, will be bounded from above and below. Furthermore, this difference approaches the energy of wave field as the Gaussian beam parameters approach their limiting values. Therefore, the quantity that we are minimizing will have at least one minimum.

One can carry out a similar analysis in 2D for the constant coefficient case as well, once again with an initial field given by a single Gaussian beam. Appendix B gives the analytic Gaussian beam solution that we use in this analysis. For the sake of a concrete example, we take the reasonable, yet arbitrary, Gaussian beam parameters for the initial field to be (see appendix B):

$$\left(a_0 = 1, y = \begin{bmatrix}0\\0\end{bmatrix} 0, \eta = \begin{bmatrix}1\\0\end{bmatrix}, \tau = -1, \beta = \begin{bmatrix}-0.9286 + 1.4121i & 0.6983 - 0.3363i\\ 0.6983 - 0.3363i & 0.8680 + 0.6538i\end{bmatrix}\right) .$$

Using this as the initial wave field that has to be decomposed, we can hold all parameters fixed, except for one and examine the energy landscape that we are minimizing in, as we did in the 1D case with y. However, instead of holding the fixed parameters at their optimal values, we perturb them randomly by a number in $[-.1, .1]$. The resulting energy landscape is shown in Figure 2. As the graph shows, in each case there is only the global minimum. While this does not prove that the global minimum is the only local minimum, it shows why the algorithm preforms well in the numerical experiments. One interesting thing to note from the figure is the plot of energy versus $\mathrm{Im}\{\beta_{12}\}$. When $\mathrm{Im}\{\beta_{12}\}$ is every negative, the imaginary part of β is no longer positive definite. The effect of this is to force a to be very small.

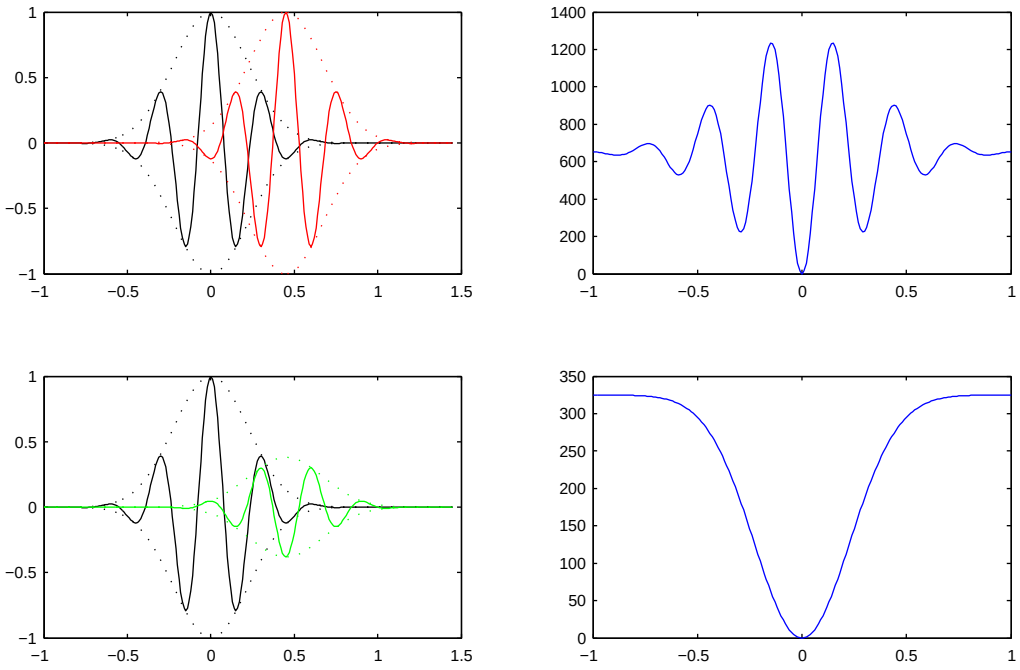

Figure 1: First graph shows the real parts of two Gaussian beams in 1D at a fixed time (the Gaussian envelopes are shown by dotted curves). Both Gaussian beams have amplitude coefficients equal to 1. To the right, the graph shows the squared energy norm of the difference between the two Gaussian beams as the location y of the second Gaussian beam in varies. The second row of graphs is the same as the first, except that the amplitude coefficient of the second Gaussian beam is given by equation (6).

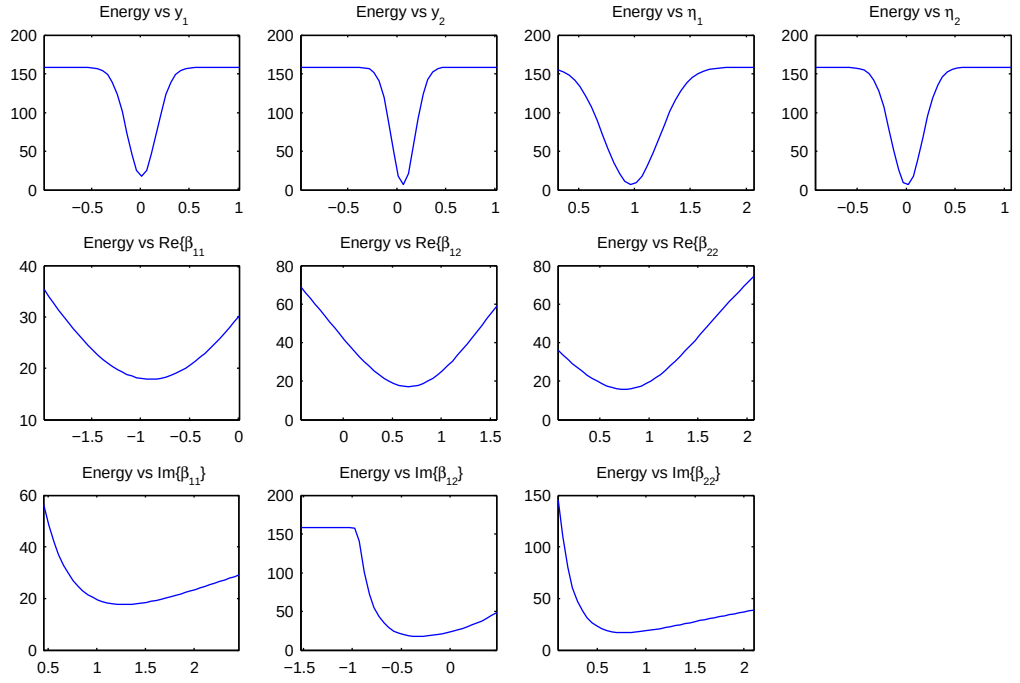

Figure 2: Plots of squared energy for two 2D Gaussian beams as each parameter for the second Gaussian beams is varied. As each parameter is varied, the rest of the parameters are held at close (but not equal) to the ideal parameters. Each graph shows that the minimum with respect to one parameter is unique.

3 Numerical Examples

We give some examples to demonstrate the decomposition method in 2D. In all of the example, the high frequency parameter $k = 50$. For the energy norm minimization (step 3 in the algorithm) we use the Nelder-Mead method. We also use the extended version of the algorithm that includes steps (a) and (b). To enforce the positive definiteness of $\mathrm{Im}\left\{D^2\phi\right\}$, we use a penalty function, which is 0 on $(1/sqrtk, \sqrt{k})$ and large otherwise.

3.1 Transmission and Reflection

In this example, we test the decomposition algorithm by decomposing a wave field that is obtained using the method of Gaussian beams. The Gaussian beam method is used to compute the wave field for reflection and transmission in the wave equation. In appendix A, we give a derivation of Gaussian beam parameters for the reflected and transmitted Gaussian beam in terms of the parameters of the incoming Gaussian beam, based only on the assumption that these three beams form a solution to the wave equation in the weak sense. The appendix is included, since it has independent value and we did not find the results in the literature, though some work in this direction was done by [3].

The experiment is performed using the initial condition given by the Gaussian beam coefficients,

$$\left(a_0 = 1, y = \begin{bmatrix} 0 \\ -0.5 \end{bmatrix}, \nabla\phi = \begin{bmatrix} 0 \\ 1 \end{bmatrix}, \phi_t = 1, D^2\phi = \begin{bmatrix} 0+i & 0 \\ 0 & 0+i \end{bmatrix}\right) .$$

The sound speed is a function of x_2 only and is equal to 3 for $x_2 < -1$ and 1 otherwise. We evolve the field using the method of Gaussian beams to $t = 1$. Then, we decompose the field using the decomposition method and obtain two sets of coefficients, one set for the transmitted wave and one set for the reflected wave. The obtained coefficients for the transmitted beam by the decomposition are

$$\left(a_0 = 0.7198 + 0.4467i, y = \begin{bmatrix} \text{-1.8106E-7} \\ \text{-1.8679} \end{bmatrix}, \nabla\phi = \begin{bmatrix} \text{8.4294E-9} \\ 0.5774 \end{bmatrix}, \phi_t = 1.0000, \right.$$
$$\left. D^2\phi = \begin{bmatrix} -0.4013 + 0.1982i & \text{3.9776E-7} - \text{5.4452E-7}i \\ \text{3.9776E-7} - \text{5.4452E-7}i & \text{-5.3503E-7} + 0.3333i \end{bmatrix}\right) ,$$

and for the reflected beam are

$$\left(a_0 = 0.2082 + \text{8.6211E-2}i, y = \begin{bmatrix} \text{-4.9143E-8} \\ \text{-0.5000} \end{bmatrix}, \nabla\phi = \begin{bmatrix} \text{-1.0294E-8} \\ \text{-1.0000} \end{bmatrix}, \phi_t = 1.000, \right.$$
$$\left. D^2\phi = \begin{bmatrix} -0.4999 + 0.5003i & \text{-2.4479E-8} - \text{7.5893E-7}i \\ \text{-2.4479E-8} - \text{7.5893E-7}i & \text{2.1258E-7} + 1.0000i \end{bmatrix}\right) .$$

The difference between these coefficients and the Gaussian beam method coefficients is on the order of 10^{-6}. This difference can be decreased by changing the stopping criteria for the Nelder-Mead method. The energy is very well represented by the extracted beams, as expected since the coefficients are almost identical, see Figure 3.

3.2 Destructive Interference

To test the ability of the algorithm to decompose complicated fields, we decompose a Gaussian beam field that exhibits strong cancellations. This field is obtained as the sum of the following 8 Gaussian beams:

$$\left(a_0 = *, y = \begin{bmatrix} 0 \\ 0 \end{bmatrix}, \nabla\phi = \begin{bmatrix} \pm 1 \\ \pm 1 \end{bmatrix}, \phi_t = \pm\sqrt{2}, D^2\phi = \begin{bmatrix} 0 + 0.75i & 0 \\ 0 & 0 + 1.25i \end{bmatrix}\right) ,$$

where every combination of '+' and '−' is taken and the '∗' is +1 if number of '−'s is even and −1 if the number of '−'s is odd. Each of these beams is different, but they are chosen in such a way so that there is extreme cancellation. Using this superposition of beams for the wavefield (f, g) that has to be decomposed, one finds that at $t = 0$, their sum f is 0, the real part of g (the time derivative at $t = 0$) is also 0. Thus all of the information is stored in the imaginary part of g. Figure 4 shows the imaginary part of g and the energy function for this data. As one can see from the plot of the energy function, at the common center $(0, 0)$, the

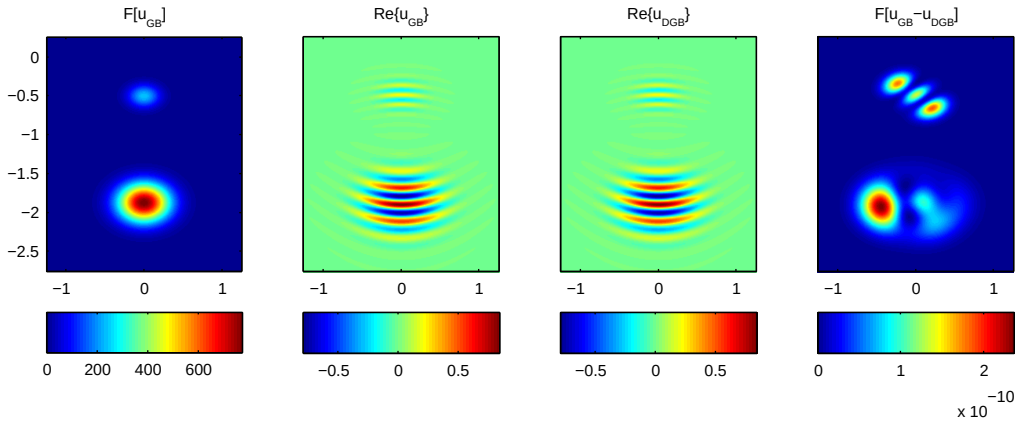

Figure 3: Wave fields and energy at $t = 1$ for the reflection and transmission example. The finite difference solution is denoted by u_{GB} and the wave field evaluated from the estimated Gaussian beam coefficients for the u_{GB} wave field is denoted by u_{DGB}. Note that the color scale for the 4th graph is very different from the 1st graph.

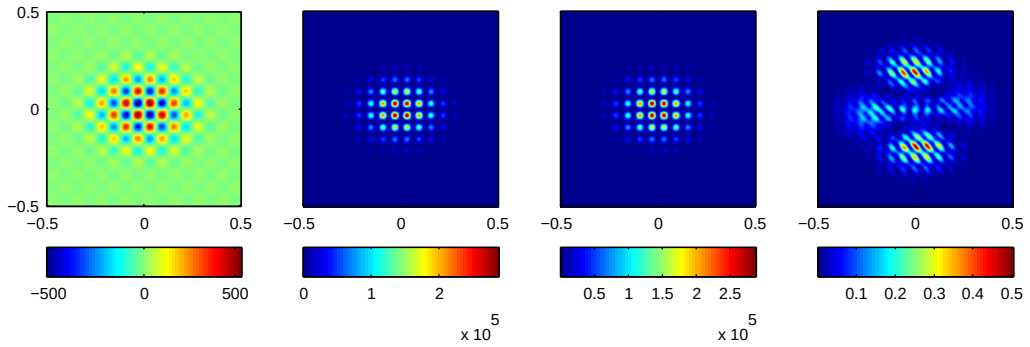

Figure 4: Wave field for the destructive interference experiment. The graphs show (from left to right) the imaginary part of g, the energy function for the initial wave field, the energy function of the wave field obtained from the superposition of the extracted Gaussian beams, and the energy function of the difference of these two fields. Note that the color scale for each graph is different.

beams cancel perfectly to give no energy. Thus, this should be a particularly difficult case for the algorithm, since it uses the energy function for the initial placement of the beams.

The results of the decomposition are showing in Figure 4. The algorithm correctly identifies that there are 8 beams and absorbs more than 99% of the energy. Figure 5, shows the energy norm difference between the wave field and the extracted Gaussian beam wave field versus the number of extracted beams.

3.3 Double Slit

In this section, we show that even in the case of crossing waves when underlying wave field is not Gaussian beam in nature, the decomposition method succeeds in extracting a Gaussian beam representation of the waves. We use a second order finite difference scheme with absorbing boundary conditions [6] to obtain the wave field to be decomposed. Figure 6 shows the sound speed and the finite difference solution. At $t = 2.0$, we take the solution in the rectangle $[-2, 2] \times [0.25, 1.75]$ and apply the decomposition method to this part of the field. The algorithm terminates after 15 Gaussian beams have been extracted. With these beams, approximately 90% of the energy has been represented. The Gaussian beams are shown in Figure 8 and the energy function is shown in Figure 9. Figure 7 shows the energy norm difference between the wave field and the extracted Gaussian beam wave field versus the number of extracted beams.

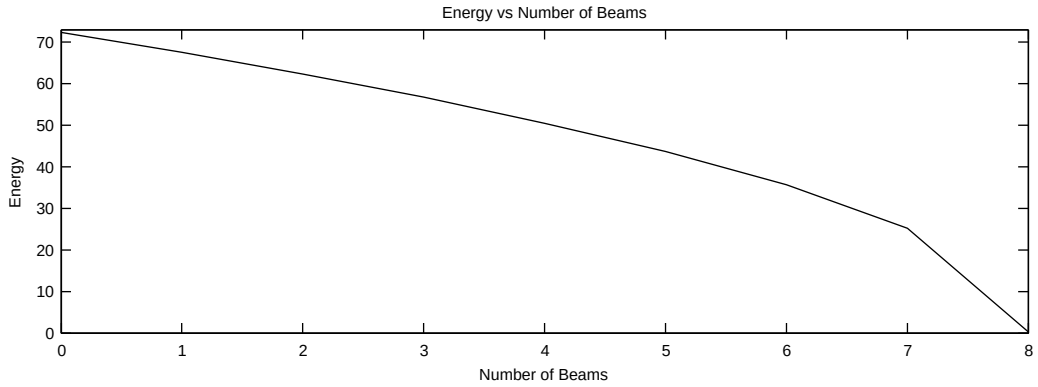

Figure 5: Energy norm difference between the wave field and the extracted Gaussian beam wave field as a function of the number of extracted beams for the destructive interference experiment.

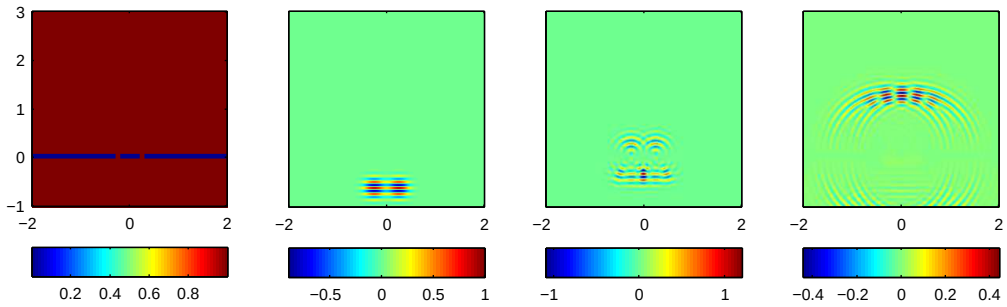

Figure 6: Wave field for the double slit experiment. The first plot shows the sound speed, then progressively from left to right, the plots show the real part of the wave field at $t = 0.0$, 1.0 and 2.0.

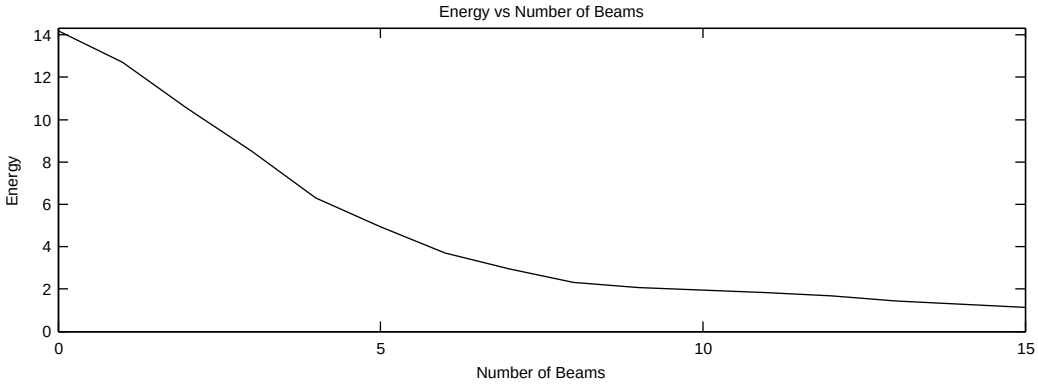

Figure 7: Energy norm difference between the wave field and the extracted Gaussian beam wave field as a function of the number of extracted beams for the double slit experiment.

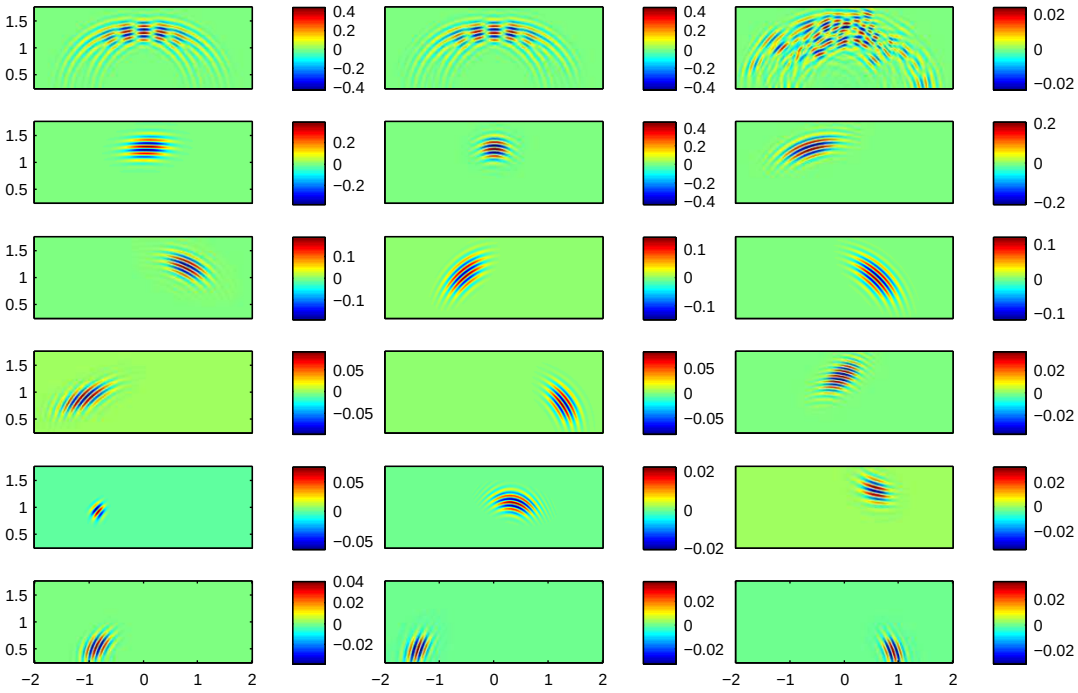

Figure 8: Gaussian beam wave fields for the double slit experiment. The top row shows (from left to right) the real part of the wave field from the finite difference, the real part of the wave field obtained from the superposition of the extracted Gaussian beams, and the difference between these two fields. The rest of the graphs are the individual Gaussian beam fields in order that the decomposition method extracted them (left to right, top to bottom). Note that the color scale for each graph is different and that the domain for each graph is $[-2, 2] \times [0.25, 1.75]$.

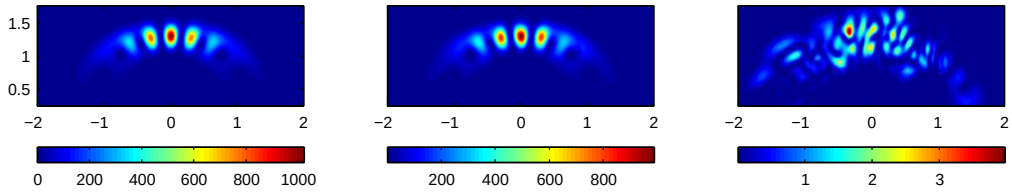

Figure 9: Gaussian beam wave energy function for the double slit experiment. The graphs show (from left to right) the energy function for the wave field from the finite difference, the energy function of the wave field obtained from the superposition of the extracted Gaussian beams, and the energy function of the difference of these two fields. Note that the color scale for the last graph is different and that the domain for each graph is $[-2, 2] \times [0.25, 1.75]$.

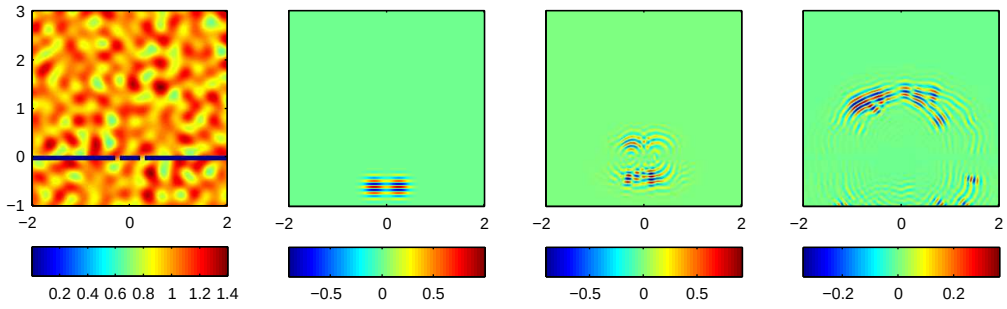

Figure 10: Wave field for the double slit experiment with variable sound speed. The first plot shows the sound speed, then progressively from left to right, the plots show the real part of the wave field at $t = 0.0$, 1.0 and 2.0.

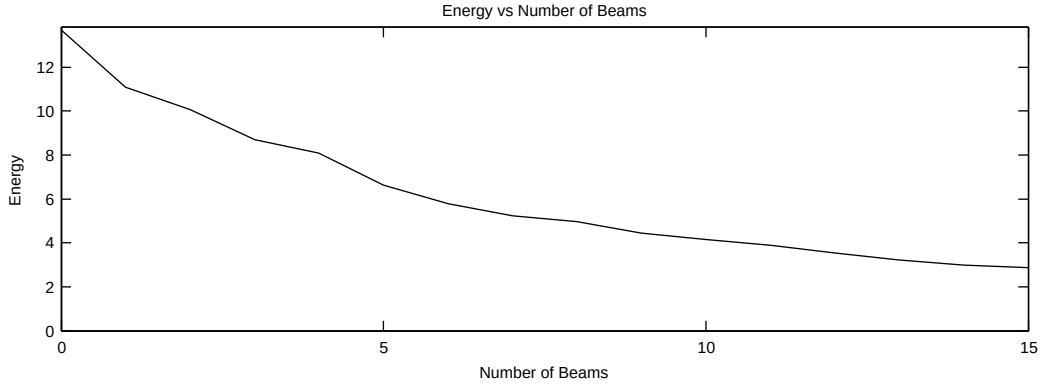

Figure 11: Energy norm difference between the wave field and the extracted Gaussian beam wave field as a function of the number of extracted beams for the double slit experiment with variable coefficients.

3.4 Double Slit with Variable Coefficients

We revisit the double slit example, but we change the sound speed to have a smooth, but randomly varying perturbation. We show the decomposition method succeeds in extracting a Gaussian beam representation of the waves. As in the previous examples, we use a second order finite difference scheme to obtain the wave field that is to be decomposed. Figure 10 shows the sound speed and the finite difference solution. As the figure shows, the waves in this example are more complicated. At $t = 2.0$, we take the solution in the rectangle $[-2, 2] \times [0.25, 1.75]$ and apply the decomposition method to this part of the field. The algorithm is terminated when 15 Gaussian beams have been extracted. With 15 beams, approximately 80% of the energy has been represented. By adding more beams, more of the energy could be represented. The Gaussian beams are shown in Figure 12 and the energy function is shown in Figure 13. Figure 11 shows the energy norm difference between the wave field and the extracted Gaussian beam wave field versus the number of extracted beams.

4 Conclusion

We have presented a method for decomposing a high frequency wave field into a superposition of Gaussian beams. The selection principle for the Gaussina beam parameters is based on approximate minimization of the energy of the difference between the given wave field and the superposition of Gaussian beams. Both numerical examples that correspond to a finite number of Gaussian beams and more general wave Fields show the efficiency of the algorithm.

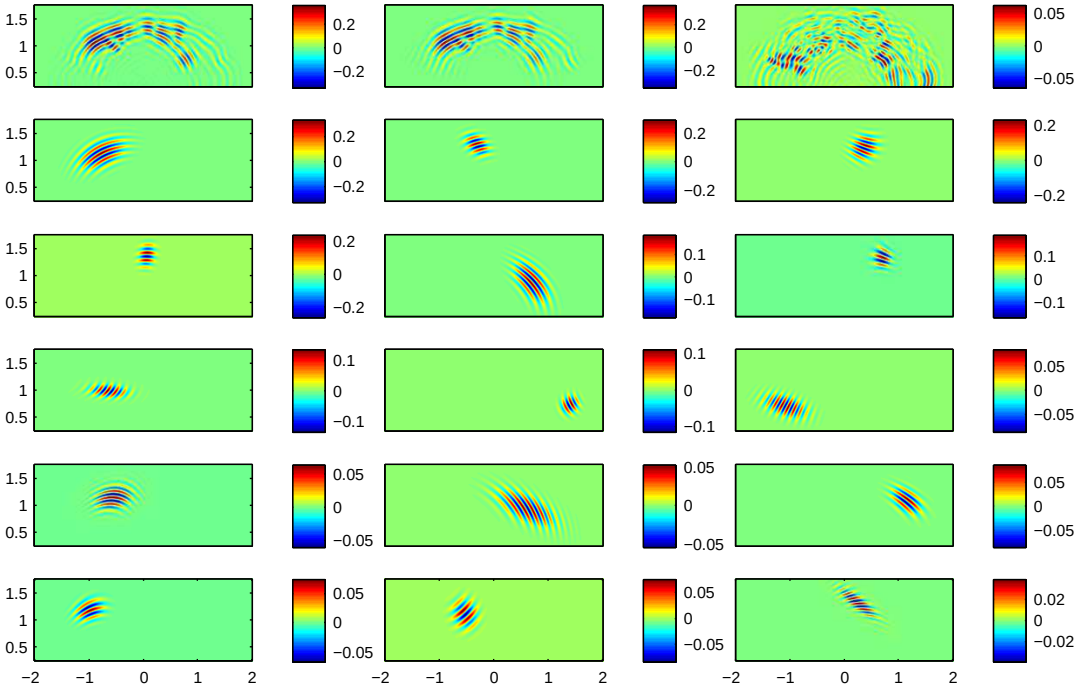

Figure 12: Gaussian beam wave fields for the double slit experiment with variable sound speed. The top row shows (from left to right) the real part of the wave field from the finite difference, the real part of the wave field obtained from the superposition of the extracted Gaussian beams, and the difference between these two fields. The rest of the graphs are the individual Gaussian beam fields in order that the decomposition method extracted them (left to right, top to bottom). Note that the color scale for each graph is different and that the domain for each graph is $[-2, 2] \times [0.25, 1.75]$.

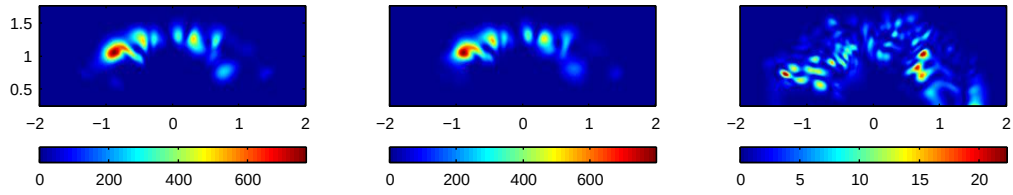

Figure 13: Gaussian beam wave energy function for the double slit experiment with variable sound speed. The graphs show (from left to right) the energy function for the wave field from the finite difference, the energy function of the wave field obtained from the superposition of the extracted Gaussian beams, and the energy function of the difference of these two fields. Note that the color scale for the last graph is different and that the domain for each graph is $[-2, 2] \times [0.25, 1.75]$.

Acknowledgments

The authors acknowledge the support of Chevron. NMT was partially supported by the NSF (UT Austin RTG Grant No. DMS-0636586 and UCLA VIGRE Grant No. DMS-0502315). RT was in part supported by an Alfred P. Sloan Fellowship.

A Transmission and Reflection of Gaussian Beams

In this section, we consider the reflection and transmission problem for Gaussian beams. Previous work in this direction has been done in [3]. This derivation is based solely on the weak formulation of the wave equation and the assumption that there is an incoming, reflected and transmitted wave.

A.1 Weak Formulation and the Matching Condition

We consider the wave equation in n space dimensions with a sound speed which is smooth up to either side of a co-dimension 1 hypersurface, Σ, but fails to be smooth across it. We assume that this surface is implicitly defined by some smooth function Ψ,

$$\Sigma = \{x : \Psi(x) = 0,\ \nabla\Psi(x) \neq 0\} \ ,$$

and that the sound speed $c(x)$ is given by

$$c(x) \quad = \quad \left\{ \begin{array}{lll} c^-(x) & \text{for} & \Psi(x) < 0 \\ c^+(x) & \text{for} & \Psi(x) > 0 \end{array} \right. \ ,$$

for c^+, $c^- \in C^\infty(\mathbb{R}^n)$. We work in the high frequency regime and treat this problem as a transmission-reflection problem. Thus, we look for solutions of the wave equation

$$u_{tt} - c(x)\triangle u \quad = \quad 0 \text{ in } \mathbb{R}_t \times \mathbb{R}^n_x \tag{7}$$

which consist of an incoming wave, a reflected wave, and a transmitted wave,

$$u \quad = \quad \left\{ \begin{array}{lll} u^I + u^R & \text{for} & \Psi(x) < 0 \\ u^T & \text{for} & \Psi(x) > 0 \end{array} \right. \ , \tag{8}$$

locally near some point $x_0 \in \Sigma$. For u to be a distribution solution of (7), we need the following equations to hold on Σ

$$\begin{aligned} u^I + u^R &= u^T \\ \nabla u^I \cdot \nu + \nabla u^R \cdot \nu &= \nabla u^T \cdot \nu \ , \end{aligned} \tag{9}$$

for ν normal to Σ.

In what follows, we will use the notation

$$\begin{aligned} f_\nu &= \sum_{j=1}^n \nu_j f_{x_j} \ , \\ f_{\nu\nu} &= \sum_{j=1}^n \sum_{k=1}^n \nu_j f_{x_j x_k} \nu_k \ , \\ \nabla^\tau f &= \nabla f - f_\nu \nu \ . \end{aligned}$$

Now, we suppose that the three waves have the same form

$$\begin{aligned} u^I &= A^I e^{ik\phi^I} = \left(a^{0I} + \frac{1}{k} a^{1I} + \ldots + \frac{1}{k^N} a^{NI} \right) e^{ik\phi^I} \ , \\ u^R &= A^R e^{ik\phi^R} = \left(a^{0R} + \frac{1}{k} a^{1R} + \ldots + \frac{1}{k^N} a^{NR} \right) e^{ik\phi^R} \ , \\ u^T &= A^T e^{ik\phi^T} = \left(a^{0T} + \frac{1}{k} a^{1T} + \ldots + \frac{1}{k^N} a^{NT} \right) e^{ik\phi^T} \ , \end{aligned}$$

with k large and the phases and amplitudes independent of k. Note that this independence of k and the matching condition equations (9) force

$$\phi^I = \phi^R = \phi^T$$

on Σ, see [4] Chapter 7, Section 7.2 for details and a physical interpretation. We assume that the incoming phase, ϕ^I, and amplitudes, a^{jI} are known and that A^I is supported near x_0. Furthermore, we assume that $\phi^I_\nu(x_0) \neq 0$ and that u^I is an asymptotically valid solution of (7) in $\Psi(x) < 0$.

A.2 Construction of the Incoming, Reflected and Transmitted Beams

We proceed as in the method of geometric optics. Substituting the form of the solution into the wave equation and equating powers of k, we get that each of the three phases ϕ^I, ϕ^R and ϕ^T has to satisfy the eikonal equation,

$$|\phi_t|^2 - c(x)|\nabla\phi|^2 \quad = \quad 0 \ ,$$

in the appropriate domain. Since $\phi^I = \phi^R = \phi^T$ on Σ, all of the tangential derivatives of the three phases will agree on Σ. Thus, after substituting, we have that on Σ,

$$\begin{aligned} |\phi^R_\nu|^2 &= |\phi^I_\nu|^2 \\ |\phi^T_\nu|^2 &= \frac{c^-|\phi^I_\nu|^2 - (c^+ - c^-)|\nabla^\tau\phi^I|^2}{c^+} \ . \end{aligned} \tag{10}$$

Since $\nabla\phi$ gives the direction of propagation, to have a reflected wave and a transmitted wave, we need

$$\begin{aligned} \phi^R_\nu &= -\phi^I_\nu \\ \phi^T_\nu &= \sqrt{\frac{c^-|\phi^I_\nu|^2 - (c^+ - c^-)|\nabla^\tau\phi^I|^2}{c^+}} \ . \end{aligned}$$

These expressions give us the last piece of information necessary to solve the eikonal equations locally for ϕ^R and ϕ^T by the method of characteristics. Also they determine the Hessian matrices of ϕ^R and ϕ^T except for $\phi^R_{\nu\nu}$ and $\phi^T_{\nu\nu}$ on Σ. We can obtain this last part by differentiating the eikonal equations in the ν direction. For each of the phases,

$$2\phi_t\phi_{t\nu} - 2c\nabla^\tau\phi\cdot\nabla^\tau\phi_\nu - 2c\phi_\nu\phi_{\nu\nu} - c_\nu|\nabla\phi|^2 \quad = \quad 0 \ ,$$

which gives,

$$\phi_{\nu\nu} \quad = \quad \frac{2\phi_t\phi_{t\nu} - c_\nu(x)|\nabla\phi|^2 - 2c\nabla^\tau\phi\cdot\nabla^\tau\phi_\nu}{2c\phi_\nu} \ . \tag{11}$$

Similarly, we can compute higher derivatives of the phases on Σ.

Now, we look at the amplitudes. To top order in k:

$$\begin{aligned} a^{0I} + a^{0R} &= a^{0T} \\ a^{0I}\phi^I_\nu + a^{0R}\phi^R_\nu &= a^{0T}\phi^T_\nu \ . \end{aligned} \tag{12}$$

Since we have already determined the ν derivatives of the phases on Σ, these equations can be used to obtain a^{0R} and a^{0T} on Σ, which serve and an initial condition for the transport equations for the highest order reflected and transmitted amplitudes:

$$2\phi_t a^0_t + \phi_{tt}a^0 - c(x)a^0\triangle\phi - 2c(x)\nabla\phi\cdot\nabla a^0 \quad = \quad 0 \ . \tag{13}$$

As in the case for the phases, we have local existence for the amplitudes, and as before we can determine the derivatives of the amplitudes on Σ by differentiating equations (12) and the transport equation (13).

The next order amplitudes satisfy

$$\begin{aligned} a^{1I} + a^{1R} &= a^{1T} \\ a^{1I}\phi^I_\nu + a^{0I}_\nu + a^{1R}\phi^R_\nu + a^{0R}_\nu &= a^{1T}\phi^T_\nu + a^{0T}_\nu \ , \end{aligned} \tag{14}$$

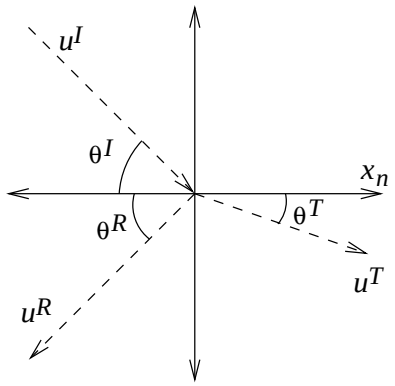

Figure 14: Incoming, reflected and transmitted Gaussian beams.

which again give the necessary initial conditions for the next order transport equations. In this fashion, we can continue until we have determined the amplitudes up to order N; thus constructing a local asymptotic solution of (7) of the form (8). We remark that these equations provide the necessary initial conditions for the construction global Gaussian beam solutions of the form (8). There is only one technical point that needs to be addressed. Since Gaussian beams determine the amplitude and phase functions up to high order in k, the matching conditions (9) will only be satisfied to a high order in $1/k$. This is not enough however, since for the form (8) to be a weak solution of the wave equation (7) the matching condition has to hold exactly. To correct this, we take the difference between the wave field for $\Psi < 0$ and $\Psi > 0$ on Σ and extend it smoothly to a function on all of $\mathbb{R}^n$. This function can then be added to the Gaussian beam solution to make it a true weak solution of the wave equation. This function will not affect the asymptotics as it is of high order in $1/k$.

A.3 Snell's Law, Total Internal Reflection, Reflection and Transmission Coefficients

Suppose that

$$c(x) = \begin{cases} c^- & \text{for} \quad x_n < 0 \\ c^+ & \text{for} \quad x_n > 0 \end{cases} .$$

Thus, ν points in the x_n direction and Σ is the hyperplane $x_n = 0$. Let ∇' be the gradient in $x_1, \ldots, x_{n-1}$ and compute

$$\begin{aligned} \phi^R_{x_n} &= -\phi^I_{x_n} \\ \phi^T_{x_n} &= \sqrt{\frac{(c^- - c^+)|\nabla'\phi^I|^2 + c^-|\phi^I_{x_n}|^2}{c^+}} , \end{aligned}$$

for $x_n = 0$. Note that the incoming, reflected and transmitted waves lie in the same plane (see Figure 14).

We calculate:

$$\begin{aligned} \sin(\theta^I) &= \frac{|\nabla'\phi^I|}{|\nabla\phi^I|} \\ \sin(\theta^R) &= \frac{|\nabla'\phi^R|}{|\nabla\phi^R|} = \frac{|\nabla'\phi^I|}{|\nabla\phi^I|} = \sin(\theta^I) \\ \sin(\theta^T) &= \frac{|\nabla'\phi^T|}{|\nabla\phi^T|} = \sqrt{\frac{c^+}{c^-}}\frac{|\nabla'\phi^I|}{|\nabla\phi^I|} = \sqrt{\frac{c^+}{c^-}}\sin(\theta^I) . \end{aligned}$$

Thus, we have obtained the familiar "angle of incidence equals angle of reflection" and Snell's law:

$$\begin{aligned} \theta^R &= \theta^I \\ \frac{\sin(\theta^T)}{\sqrt{c^+}} &= \frac{\sin(\theta^I)}{\sqrt{c^+}} . \end{aligned}$$

Total internal reflection occurs when $\phi^T_{x_n}$ is complex, as in that case the transmitted wave just decays exponentially in x_n:

$$\begin{aligned}\frac{(c^- - c^+)|\nabla'\phi^I|^2 + c^-|\phi^I_{x_n}|^2}{c^+} &\leq 0\\ c^-|\nabla\phi^I|^2 &\leq c^+|\nabla'\phi^I|^2\\ \sqrt{\frac{c^-}{c^+}} &\leq \sin(\theta^I)\ .\end{aligned}$$

Thus the critical angle for total internal reflection is

$$\arcsin\left(\sqrt{\frac{c^-}{c^+}}\right)\ .$$

Note that for total internal reflection to occur $c^- < c^+$.

The reflection and transmission coefficients measure what fraction of the incident amplitude is transmitted and what fraction is reflected. From (12), we readily compute:

$$\begin{aligned}a^{0R} &= \frac{\phi^I_{x_n}/\phi^T_{x_n} - 1}{1 + \phi^I_{x_n}/\phi^T_{x_n}}\ a^{0I} \equiv Ra^{0I}\\ a^{0T} &= \frac{2}{1 + \phi^T_{x_n}/\phi^I_{x_n}}\ a^{0I} \equiv Ta^{0I}\ .\end{aligned}$$

At normal incidence (ie $|\nabla\phi^I|^2 = |\phi^I_{x_n}|^2$), the transmission and reflection coefficients become

$$\begin{aligned}R &= \frac{\sqrt{c^+/c^-} - 1}{1 + \sqrt{c^+/c^-}} = \frac{\sqrt{c^+} - \sqrt{c^-}}{\sqrt{c^-} + \sqrt{c^+}}\\ T &= \frac{2}{1 + \sqrt{c^-/c^+}} = \frac{2\sqrt{c^+}}{\sqrt{c^-} + \sqrt{c^+}}\ .\end{aligned}$$

B Analytic Gaussian Beams Solutions of the Constant Coefficient Wave Equation

For the constant coefficient wave equation, one can find analytic Gaussian beam solutions, since the ordinary differential equations that define the beam have a simple form. In 1D, since any function of $x-t$ or $x+t$ will satisfy the wave equation, any Gaussian beam solution can be written as

$$a_0 e^{ik\left[\xi_0(x-x_0\pm t)+\beta(x-x_0\pm t)^2/2\right]}\ ,$$

where a_0, x_0, ξ_0 and β are the parameters that define the Gaussian beam (note that $\mathrm{Im}\{\beta\}$ has to be greater then 0).

In 2D, we can also derive the analytic solution. We begin by looking at the equations that define the characteristic rays. In the 2D constant coefficient ($c(x) = 1$), the ray tracing system of ODEs will have the following solution:

$$\begin{aligned}\mathcal{T}(s) &= 2\tau s\\ \mathcal{X}(s) &= -2\eta s + y\\ \tau(s) &= \pm|\eta|\\ \xi(s) &= \eta\ ,\end{aligned}$$

where s is the ray parameter, $\eta = (\eta_1, \eta_2)$ is the initial $\nabla\phi$ and $y = (y_1, y_2)$ is the initial Gaussian beam center. The eikonal equation gives $\tau = \pm|\eta|$. As expected, the characteristic rays are straight lines. Since $\mathcal{T}(s) = t$, we have $s = t/(2\tau)$ and thus the characteristic rays can be expressed as functions of time.

With the aid of Mathematica, one can also solve the ODEs that define $D^2\phi$ along the characteristics,

$$\begin{aligned} M_{11}(t) &= \frac{t\beta_{12}^2\eta_1^2 + \beta_{11}\tau^3 - t\beta_{11}\beta_{22}\eta_1^2}{\tau^3 - t(\beta_{11}\eta_2^2 - 2\beta_{12}\eta_1\eta_2 + \beta_{22}\eta_1^2)} \\ M_{12}(t) &= \frac{t\beta_{12}^2\eta_1\eta_2 + \beta_{12}\tau^3 - t\beta_{11}\beta_{22}\eta_1\eta_2}{\tau^3 - t(\beta_{11}\eta_2^2 - 2\beta_{12}\eta_1\eta_2 + \beta_{22}\eta_1^2)} \\ M_{22}(t) &= \frac{t\beta_{12}^2\eta_2^2 + \beta_{22}\tau^3 - t\beta_{11}\beta_{22}\eta_2^2}{\tau^3 - t(\beta_{11}\eta_2^2 - 2\beta_{12}\eta_1\eta_2 + \beta_{22}\eta_1^2)} \ , \end{aligned}$$

where the subscripts denote the type of second derivative coefficient (M_{12} is the $\partial x_1 \partial x_2$-derivative) and β is the initial Hessian matrix $D^2\phi$. Note that $\mathrm{Im}\{\beta\}$ must be a positive definite matrix.

Similarly, one computes the amplitude of the Gaussian beam:

$$A(t) = a_0\sqrt{\frac{\tau^3}{\tau^3 - t(\beta_{11}\eta_2^2 - 2\beta_{12}\eta_1\eta_2 + \beta_{22}\eta_1^2)}} \ ,$$

with the branch of the square root taken so that $A(0) = a_0$.

Thus we have expressed the Gaussian beam as function of (x_1, x_2, t) with parameters (a_0, y, η, β) and the sign of τ:

$$A(t)e^{ik\left[\eta\cdot(x-\mathcal{X}(t))+\frac{1}{2}\left(M_{11}(t)(x_1-\mathcal{X}_1(t))^2+2M_{12}(t)(x_1-\mathcal{X}_1(t))(x_2-\mathcal{X}_2(t))+M_{22}(t)(x_2-\mathcal{X}_2(t))^2\right)\right]} \ ,$$

with the abuse of notation, $\mathcal{X}(t) = -\eta t\tau + y$.

Finally, we note that in the case parameters given by

$$\left(a_0 = 1, y = \begin{bmatrix}0\\0\end{bmatrix}, \eta = \begin{bmatrix}0\\\frac{1}{2}\end{bmatrix}, \tau = -\frac{1}{2}, \beta = \begin{bmatrix}ia & 0\\0 & ib\end{bmatrix}\right) \ ,$$

this solution reduces to the special solution derived in [14],

$$\sqrt{\frac{1}{1+2iat}}\exp\left[ik\left(\frac{1}{2}(x_2-t) + \frac{1}{2}\left(ib(x_2-t)^2 + \frac{ia+2a^2t}{1+4a^2t^2}x_1^2\right)\right)\right] \ .$$

References

[1] Jean-David Benamou, Francis Collino, and Olof Runborg. Numerical microlocal analysis of harmonic wavefields. *J. Comput. Phys.*, 199(2):717–741, 2004.

[2] V. Červený, M. Popov, and I. Pšenčík. Computation of wave fields in inhomogeneous media - Gaussian beam approach. *Geophys. J. R. Astr. Soc.*, 70:109–128, 1982.

[3] V. Červený and I. Pšenčík. Gaussian beams in elastic 2-D laterally varying layered structures. *Geophys. J. Int.*, 78:65–91, 1984.

[4] F. S. Crawford. *Waves*, volume 3 of *The Berkeley Physics Course*. McGraw-Hill, 1968.

[5] Björn Engquist, Sergey Fomel, Nicolay Tanushev, and Richard Tsai. Gaussian beam decomposition with application to exploration seismology. *to appear*.

[6] Björn Engquist and Andrew Majda. Absorbing boundary conditions for the numerical simulation of waves. *Math. Comp.*, 31(139):629–651, 1977.

[7] Björn Engquist and Olof Runborg. Computational high frequency wave propagation. *Acta Numer.*, 12:181–266, 2003.

[8] Samuel H. Gray and Norman Bleistein. True-amplitude gaussian-beam migration. *Geophysics*, 74(2):S11–S23, 2009.

[9] N. R. Hill. Gaussian beam migration. *Geophysics*, 55(11):1, 1990.

[10] N. R. Hill. Prestack Gaussian-beam depth migration. *Geophysics*, 66(4):1240–1250, 2001.

[11] Joseph B. Keller. Geometrical theory of diffraction. *J. Opt. Soc. Amer.*, 52:116–130, 1962.

[12] L. Klimeš. Expansion of a high-frequency time-harmonic wavefield given on an initial surface into Gaussian beams. *Geophys. J. R. Astr. Soc.*, 79:105–118, 1984.

[13] J. A. Nelder and R. Mead. A simplex method for function minimization. *Comput. J.*, 7(4):308–313, January 1965.

[14] James Ralston. Gaussian beams and the propagation of singularities. In *Studies in partial differential equations*, volume 23 of *MAA Stud. Math.*, pages 206–248. Math. Assoc. America, Washington, DC, 1982.

[15] Nicolay M. Tanushev. Superpositions and higher order Gaussian beams. *Commun. Math. Sci.*, 6(2):449–475, 2008.

[16] Nicolay M. Tanushev, Jianliang Qian, and James V. Ralston. Mountain waves and Gaussian beams. *Multiscale Model. Simul.*, 6(2):688–709, 2007.

[17] K. Žáček. Decomposition of the wave field into optimized Gaussian packets. *Stud. Geophys. Geod.*, 50(3):367–380, July 2006.